THERMALLY DRIVEN GAS FLOWS IN CAVITIES FAR FROM LOCAL EQUILIBRIUM

Giorgos Tatsios[1], Dimitris Valougeorgis[1] and Stefan K. Stefanov[2]

[1]Department of Mechanical Engineering
University of Thessaly
Volos, GR-38334, Greece
e-mail: tatsios@mie.uth.gr; diva@mie.uth.gr

[2]Institute of Mechanics
Bulgarian Academy of Sciences
Sofia, Bulgaria
e-mail: stefanov@imbm.bas.bg

Keywords: Kinetic Theory, Rarefied Gas Dynamics, DSMC, Knudsen Number, GASMEMS.

Abstract. *The flow of a rarefied gas confined in a two dimensional cavity due to non-isothermal walls is investigated. Two set-ups of boundary conditions are considered. In the first case the top and bottom walls are kept at constant temperatures and a linear temperature distribution is applied along the lateral walls and in the second case three walls are kept at constant low temperatures and the fourth one is heated. Since the flow is far from local equilibrium in a wide range of the Knudsen number, a kinetic approach based on the Bolltzmann equation is required. The flow is simulated by the deterministic solution of the Shakhov kinetic model and stochastically by implementing the DSMC method. Although the investigated flow configuration is simple, it is rich in non-equilibrium phenomena.*

1 INTRODUCTION

Rarefied gas flows are characterized by conditions far from local equilibrium. The measure of the departure from equilibrium is the Knudsen number, denoted as Kn, which is defined as the ratio of the mean free path over a characteristic length of the problem. For $Kn > 0.1$, i.e., when the flow is in the so-called transition and free molecular regimes, the traditional Navier-Stokes-Fourier approach is no longer valid, and a more fundamental kinetic type approach should be applied.

Such flows have lately received considerable attention due to their theoretical interest and their implementation in several emerging technological fields including vacuum packed MEMS [1], micropumps/microactuators [2,3] and vacuum systems [4]. They are also commonly applied in benchmarking of novel numerical schemes [5,6,7]. In the present work a review of some recent developments in temperature driven rarefied gas flows in cavities subject to two different boundary condition cases is presented. The first case concerns a cavity where the top and bottom walls are kept at constant temperatures, while a linear temperature distribution between those temperatures is applied at the lateral walls [8]. In the second case the three walls are kept at constant low temperatures while the fourth is heated by a given heat flux distribution [9]. Modeling is based on the non-linear Shakhov model [10], while the DSMC method [11] is used for benchmarking purposes.

2 FLOW CONFIGURATION

A rarefied monatomic gas is confined in a 2D enclosure of side length W. The physical space variables are denoted by (x', y') with $-W/2 < x' < W/2$ and $0 < y' < W$. Due to the temperature difference of the bounding walls a steady-state heat flow through the enclosure is developed defined by the heat flux vector $\boldsymbol{Q} = \left[Q_x(x', y'), Q_y(x', y')\right]$ and due to non-equilibrium (rarefied) phenomena a flow field is also developed, defined by the velocity vector $\boldsymbol{U} = \left[U_x(x', y'), U_y(x', y')\right]$. It is noted that in rarefied flow configurations, as the present ones, gravitational forces are commonly neglected. The gas temperature and number density are denoted as $T(x', y')$ and $N(x', y')$ respectively, while the pressure is given by the equation of state $P = Nk_B T$, where k_B is the Boltzmann constant.

At this point it is convenient to introduce the following dimensionless quantities:

$$x=\frac{x'}{W},\quad y=\frac{y'}{W},\quad n=\frac{N'}{N_0},\ \tau=\frac{T'}{T_0},\quad p=\frac{P}{P_0},\quad u_x=\frac{U_x}{\upsilon_0},\quad u_y=\frac{U_y}{\upsilon_0},\quad q_x=\frac{Q_x}{P_0\upsilon_0},\quad q_y=\frac{Q_y}{P_0\upsilon_0} \tag{1}$$

The dimensionless physical space variables are $x\in\left[-1/2,1/2\right]$, $y\in\left[0,1\right]$ and the quantities n, τ, p, $\left(u_x,u_y\right)$ and $\left(q_x,q_y\right)$ are the distributions of the dimensionless number density, temperature, pressure, velocity and heat flux respectively. The reference quantities are denoted by the subscript zero. The reference pressure is $P_0=N_0k_BT_0$ and the most probable molecular speed is $\upsilon_0=\sqrt{2k_BT\ /m}$, where m is the molecular mass. The hard sphere model is used to model intermolecular collisions, providing for the viscosity the expression $\mu=\mu_0\sqrt{\tau}$ where μ_0 is the viscosity at reference temperature T_0. The flow parameter characterizing the flow is the reference Knudsen number, defined as

$$Kn_0=\frac{\sqrt{\pi}}{2}\frac{\mu_0\upsilon_0}{P_0W} \tag{2}$$

The two boundary condition cases are distinguished:

Case 1: the top and bottom walls are kept at constant temperatures T_1 and T_2 respectively with $T_1<T_2$ and a linear temperature distribution of the form $T_S=T_2-\left(T_2-T_1\right)y'/W$ is applied at the lateral walls. So, apart from the reference Knudsen number, the other parameter characterizing the flow is the temperature ratio T_1/T_2. In this case the temperature of the hot wall is used as the reference temperature ($T_0=T_2$). The average number density in the enclosure is N_0 and P_0 is taken from the equation of state.

Case 2: three walls are kept at a constant temperature T_C and the forth is heated by a constant heat flux of magnitude Q_H. In this case the second parameter characterizing the flow is the dimensionless applied heat flux $q_H=Q_H/\left(P_0\upsilon_0\right)$. The reference temperature in this case is the average temperature of the heated wall, while the reference number density and pressure are taken as in case 1.

3 DETERMINISTIC AND STOCHASTIC MODELING

3.1 Deterministic modeling

The deterministic modeling is based on the direct solution of the dimensionless Shakhov model equation. Also, the well-known projection procedure can be written as [8,9]

$$\zeta_x\frac{\partial\varphi}{\partial x}+\zeta_y\frac{\partial\varphi}{\partial y}=\frac{\sqrt{\pi}}{2}\frac{1}{Kn_0}n\sqrt{\tau}\left(\varphi^S-\varphi\right),\quad \zeta_x\frac{\partial\psi}{\partial x}+\zeta_y\frac{\partial\psi}{\partial y}=\frac{\sqrt{\pi}}{2}\frac{1}{Kn_0}n\sqrt{\tau}\left(\psi^S-\psi\right). \tag{3}$$

with $\left(\zeta_x,\zeta_y\right)$ denoting the two components of the molecular velocity vector and

$$\varphi^S=\varphi^M\left[1+\frac{4}{15}\frac{1}{n\tau^2}\left[q_x\left(\zeta_x-u_x\right)+q_y\left(\zeta_y-u_y\right)\right]\left(\left[\left(\zeta_x-u_x\right)^2+\left(\zeta_y-u_y\right)^2\right]/\tau-2\right)\right]. \tag{4}$$

$$\psi^S=\psi^M\left[1+\frac{4}{15}\frac{1}{n\tau^2}\left[q_x\left(\zeta_x-u_x\right)+q_y\left(\zeta_y-u_y\right)\right]\left(\left[\left(\zeta_x-u_x\right)^2+\left(\zeta_y-u_y\right)^2\right]/\tau-1\right)\right]. \tag{5}$$

while the reduced local Maxwellians are

$$\varphi^M=\frac{n}{\pi\tau}\exp\left[-\left[\left(\zeta_x-u_x\right)^2+\left(\zeta_y-u_y\right)^2\right]/\tau\right],\quad \psi^M=\frac{n}{2\pi}\exp\left[-\left[\left(\zeta_x-u_x\right)^2+\left(\zeta_y-u_y\right)^2\right]/\tau\right]. \tag{6}$$

The macroscopic quantities of practical interest are then taken as moments of the two reduced distribution functions φ and ψ:

$$n\left(x,y\right)=\int_{-\infty}^{\infty}\int_{-\infty}^{\infty}\varphi d\zeta_xd\zeta_y,\quad u_x\left(x,y\right)=\frac{1}{n}\int_{-\infty}^{\infty}\int_{-\infty}^{\infty}\zeta_x\varphi d\zeta_xd\zeta_y,\quad u_y\left(x,y\right)=\frac{1}{n}\int_{-\infty}^{\infty}\int_{-\infty}^{\infty}\zeta_y\varphi d\zeta_xd\zeta_y. \tag{7}$$

$$\tau(x,y)=\frac{2}{3n}\int_{-\infty}^{\infty}\int_{-\infty}^{\infty}\left[\left(\zeta_x^2+\zeta_y^2\right)\varphi+\psi\right]d\zeta_x d\zeta_y-\frac{2}{3}\left(u_x^2+u_y^2\right). \tag{8}$$

$$\boldsymbol{q}(x,y)=\left(q_x,q_y\right)=\int_{-\infty}^{\infty}\int_{-\infty}^{\infty}\left[\left[\left(\zeta_x-u_x\right)^2+\left(\zeta_y-u_y\right)^2\right]\varphi+\psi\right]\left(\boldsymbol{\zeta}-\boldsymbol{u}\right)d\zeta_x d\zeta_y . \tag{9}$$

The purely diffuse Maxwell boundary conditions have been implemented and the outgoing distributions at the boundaries denoted by φ^+ and ψ^+, are expressed as

$$\varphi^+=\frac{n_w}{\pi\tau_w}\exp\left[-\left(\zeta_x^2+\zeta_y^2\right)/\tau_w\right],\quad \psi^+=\frac{n_w}{2\pi}\exp\left[-\left(\zeta_x^2+\zeta_y^2\right)/\tau_w\right]. \tag{10}$$

where n_w is a parameter calculated in terms of the ingoing distribution, satisfying the impermeability conditions and τ_w is the imposed dimensionless wall temperature. In Case 2, at the heated wall, τ_w is part of the solution and the problem closes by applying the constraint $q_y(x,0)=q_H$. Here, without loss of generality, the bottom wall is considered as the heated wall and these parameters are defined by the expressions [9]

$$\tau_w=\frac{1}{2}\left(\frac{B-q_H}{A}\right),\quad n_w=-2A\left(\frac{\pi}{\tau_w}\right)^{1/2}, \tag{11}$$

where

$$A=\int_{-\infty}^{0}\int_{-\infty}^{\infty}\zeta_y\varphi^- d\zeta_x d\zeta_y ,\quad B=\int_{-\infty}^{0}\int_{-\infty}^{\infty}\left[\left[\left(\zeta_x-u_x\right)^2+\left(\zeta_y-u_y\right)^2\right]\varphi^-+\psi^-\right]\left(\zeta_y-u_y\right)d\zeta_x d\zeta_y \tag{12}$$

with φ^- and ψ^- denoting the ingoing distribution.

The above set of integro-differential equations (3-6) coupled with the expressions (7-9) subject to boundary conditions (10-12) are solved numerically discretizing the physical space by a control volume approach and the molecular velocity space by the so-called discrete velocity method. The iterative process of the algorithm is terminated when a convergence criteria of the from

$$\varepsilon^{(k)}=\max_{i,j}\left\{\left|n_{i,j}^{(k)}-n_{i,j}^{(k-1)}\right|+\left|u_{xi,j}^{(k)}-u_{xi,j}^{(k-1)}\right|+\left|u_{yi,j}^{(k)}-u_{yi,j}^{(k-1)}\right|+\left|\tau_{i,j}^{(k)}-\tau_{i,j}^{(k-1)}\right|\right\}\le 10^{-10}. \tag{13}$$

is fulfilled. In the above expression k denotes the iteration index and $\varepsilon^{(k)}$ the error after k iterations.

3.2 Stochastic modeling

Stochastic modeling is based on the DSMC method, described in [11]. In this method the real process of particle motion is divided into two steps, the ballistic motion of the particles over a distance proportional to their velocities, which is purely deterministic and the collisions between particles that is done in a stochastic manner, following the traditional No Time Counter (NTC) scheme [11] together with the HS molecular interaction model. The implementation of the given heat flux boundary condition for case 2 is described in [12]. The interaction of the particles with the solid boundaries is purely diffuse. The physical domain is divided into 100×100 square cells with a size smaller than the mean free path, while 10^5-10^6 model particles are used and the time step is chosen to be about $1/3$ of the cell transversal time. The sampling of the macroscopic properties starts after the steady state has been achieved and carried out by volume base averaging for over $(5-15)\times10^5$ time steps giving a sample size of approximately 10^9-10^{10} samples per cell, which is sufficiently large to reduce the statistical scatter.

4 RESULTS AND DISCUSION

Results are presented for both cases, starting with Case 1. Simulations have been conducted in a wide range of Knudsen numbers and temperature ratios. More specifically, these parameters vary as $0.01<Kn_0<10$ and $0.1<T_1/T_2<0.9$. The effect of the gas rarefaction and the temperature ratio on the flow field can be seen in Fig. 1, where the streamlines and temperature contours are shown for values of the Knudsen number covering the transition to free molecular regimes and for small and large temperature differences. We observe that a stratified

temperature field is developed in all cases. In Figs. 1 (a) and (c), in the early transition regime, the whole flow domain is covered by vortices that near the lateral walls have a velocity heading from cold-to-hot regions. This behavior is expected, as the leading mechanism for this flow is thermal transpiration or creep, which leads to motion from cold to hot. What is very interesting is that for larger degrees of rarefaction Figs. 1 (b) and (d) those vortices have been squeezed and two more vortices appear, counter-rotating to them having velocities in the vicinity of the lateral walls from hot-to-cold regions, contrary to thermal creep flow. The formation of these vortices as well as the mechanism of their creation, have been extensively studied in [8]. It is concluded that this hot-to-cold flow along the lateral walls are due to the interplay between the ballistic and collision motion of the particles. Moreover, as the temperature difference is increased those unexpected flow structures expand covering larger parts of the enclosure, while for small temperature differences they are restricted close to the lateral walls.

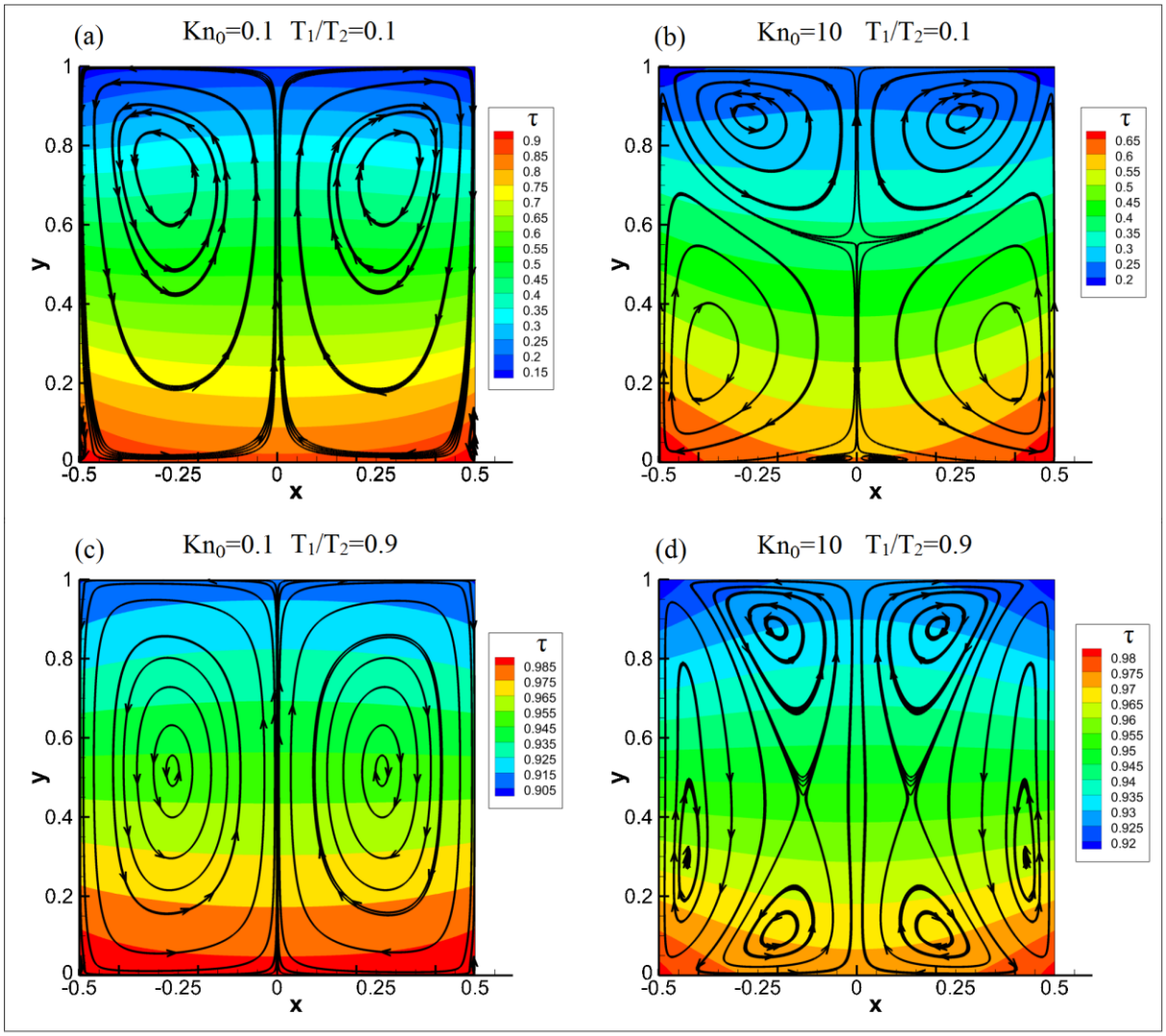

Figure 1. Streamlines and temperature contours in a square enclosure for $T_1/T_2 = 0.1, 0.9$ and $Kn_0 = 0.1, 10$ (case 1).

More information regarding the flow field near the lateral walls can be taken from Fig. 2, where the tangential velocity u_y along the lateral walls is given for small and large temperature differences and various values of the Knudsen number, ranging from the slip up to the free molecular regimes. For both temperature ratios when the Knudsen number is small $(Kn_0 = 0.01)$ the direction of the velocity on the whole lateral walls is from cold-to-hot, indicated by $(u_y < 0)$ and as the Knudsen number is increased some regions start having positive tangential velocities. For $Kn_0 = 1$ and 10 (transitional and free molecular regimes respectively) along the lateral wall there are only positive tangential velocities. Of course as $Kn_0 \to \infty$ all motion in the enclosure vanishes [13].

The flow field structure for Case 2 has qualitative similarities with that of Case 1. Again two kinds of vortices

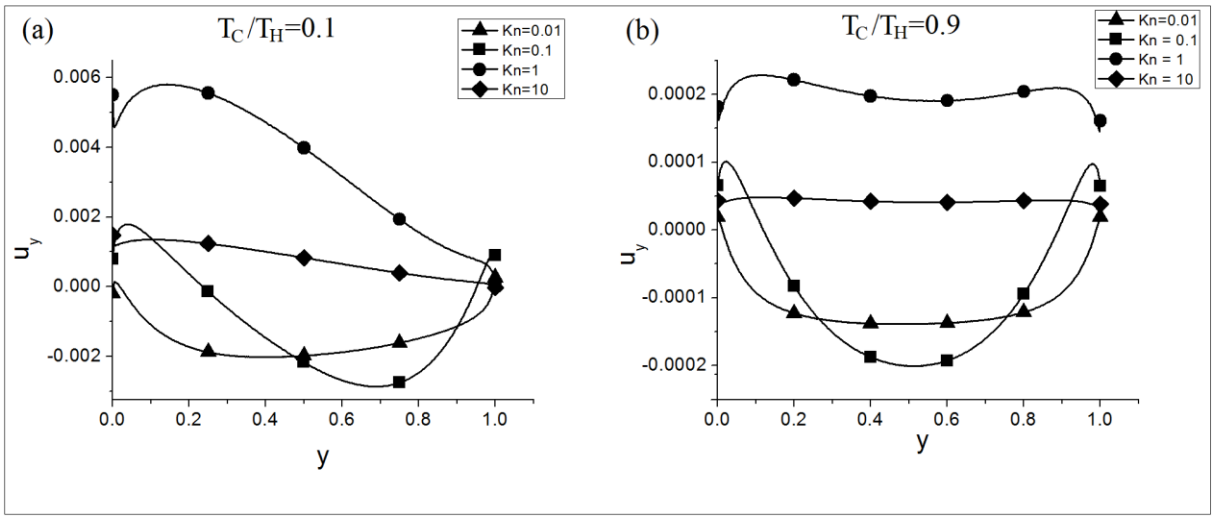

Figure 2. Tangential velocity u_y along the lateral walls of a square enclosure for $T_1/T_2 = 0.1, 0.9$ and various values of the Knudsen number (case 1).

appear along the boundaries depending on the Knudsen number and the temperature ratios (here the temperature ratio is defined in terms of the mean temperature of the heated wall). Some quantitative differences however exist, mainly in the temperature distributions due to the different boundary conditions. Case 2 configuration is close to the set-up of cooling devices in packed MEMS. Therefore, the most important results are regarding the heat flux departing from the bottom plate. As the heat flux departing from the bottom plate is given, the temperature distribution along the heated wall is part of the solution. In order to investigate the results it is convenient to introduce the average temperature of the heated wall as $\bar{T}_H = \int_{-W/2}^{W/2} T_H(x')dx'$. In Fig. 3, the temperature ratio $T_C/\bar{T}_H$ is given in terms of the applied heat flux for various values of the reference Knudsen number. A very interesting result is that for all values of the Knudsen number simulated, covering the slip, transition and free molecular regimes, for any given value of q_H, two values of the temperature ratio $T_C/\bar{T}_H$ may be obtained. More specifically as $T_C/\bar{T}_H$ is initially increased q_H is also increased, until a maximum value around $T_C/\bar{T}_H = 0.3$ and then if we further increase the temperature ratio q_H is decreased. So the heat flux has a non-monotonous behavior with respect to the temperature ratio. This is in agreement with previously reported results and a detailed explanation of this phenomenon is provided in [9].

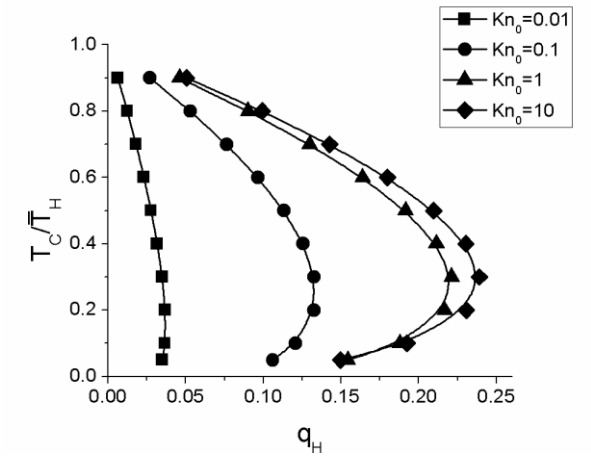

Figure 3. Temperature ratio $T_C/\bar{T}_H$ in terms of the dimensionless heat flux q_H for various values of the reference Knudsen number.

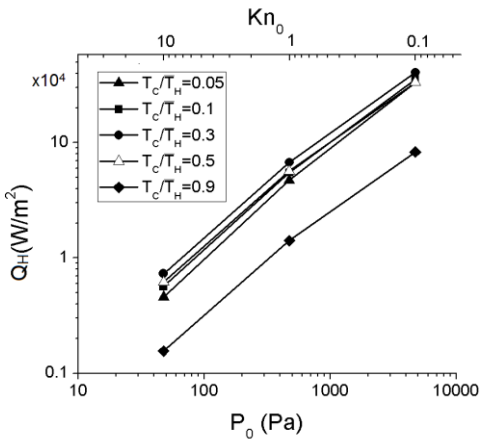

Figure 4. Departing heat flux $Q_H\left[W/m^2\right]$ from the bottom plate in terms of reference pressure for various temperature ratios.

Some indicative dimensional results are presented in Fig. 4, where the dimensional heat flux given at the bottom plate $Q_H\left[W/m^2\right]$ is plotted in terms of the reference pressure $P_0\left[Pa\right]$ for various values of the temperature ratio $T_C/\bar{T}_H$. The results are for a square cavity of side $W=50\mu m$ and the average temperature of the heated wall is $\bar{T}_H=10^3K$. The working gas is Argon $\left(m=39.95Kg/kmol\right)$. We see that for any given temperature ratio as the pressure is increased the heat flux is also increased. Moreover at any given pressure, as the temperature difference increases the heat flux also increases until it reaches a maximum value for $T_C/\bar{T}_H=0.3$, and then it decreases if the temperature difference is increased. This result is important in the stability and efficiency optimization of cooling devices operating under vacuum conditions

5 CONCLUSIONS

The thermally driven flow of a monatomic rarefied gas confined in a 2D enclosure far from local equilibrium has been investigated using both deterministic and stochastic modeling. Very good agreement between the two approaches is taken. Two boundary condition scenarios were investigated, the first having mainly scientific importance, while the second is of more of practical importance as it corresponds to cooling applications. A non-expected flow near the lateral walls contrary to the expected thermal creep flow is observed. A non-monotonic behavior of the heat flux departing from the bottom plate has been observed with the heat flux attaining a maximum value at an intermediate temperature ratio. This result is important for the optimization of cooling devices operating under rarefied conditions. It is believed that this work is of both scientific and technological interest.

REFERENCES

[1] Liu, H., Wang, M., Wang, J. and Zhang, X. (2007), "Monte Carlo simulations of gas flow and heat transfer in vacuum packed MEMS devices", *Applied Thermal Engineering*, Vol. 27, 323-329.

[2] Aleexenko, A., Gimelshein, S., Muntz, E. and Ketsdever, A. (2006), "Kinetic modeling of temperature driven flows in short microchannels", *International Journal of Thermal Sciences*, Vol. 45, 1045-1051.

[3] Ketsdever, A., Gimelshein, N., Gimelshein, S. and Selden, N. (2012), "Radiometric phenomena: From the 19th to the 21st century", *Vacuum*, Vol. 86, 1644-1662.

[4] Vargas, M., Wüest, M. and Stefanov, S. (2012), "Monte Carlo analysis of thermal transpiration effects in capacitance diaphragm gauges with helicoidal baffle system", *Journal of Physics:* Conference 362, 012013.

[5] Masters, N., D. and Ye, W. (2007), "Octant flux splitting information preservation DSMC method for thermally driven flows", *J. Comput. Phys*., Vol. 226, 2044–2062.

[6] Rana, A., Torrilhon, M. and Struchtrup, H. (2012), "Heat transfer in micro devices packaged in partial vacuum," *J. Phys.*: Conf. Ser. 362, 012034 .

[7] Huang, J. C., Xu, K. and Yu, P. (2013), "A unified gas-kinetic scheme for continuum and rarefied flows III: Microflow simulations," *Commun. Comput. Phys*., Vol. 14(5), 1147–1173.

[8] Vargas, M., Tatsios, G., Valougeorgis, D. and Stefanov, S. (2014), "Rarefied gas flow in a rectangular enclosure induced by non-isothermal walls", *Physics of Fluids*, Vol. 26, 057101.

[9] Tatsios, G., Vargas, M., Valougeorgis, D. and Stefanov, S. (2015), "Non-equilibrium gas flow and heat transfer in a heated square microcavity", *Heat Transfer Engineering, in press*.

[10] Shakhov, E. M. (1968), "Generalization of the Krook kinetic relaxation equation", *Fluid Dynamics*, Vol. 3 (5), 142-145.

[11] Bird, G. A. (1994), *Molecular Gas Dynamics and the Direct Simulation of Gas Flows*, Oxford: Clarendon Press.

[12] Akhlaghi, H., Roohi, E. and Stefanov, S. (2012), "A new iterative wall heat flux specifying technique in DSMC for heating/cooling simulations of MEMS/NEMS", *International Journal of Thermal Sciences*, Vol. 59, 111-125.

[13] Sone, Y. (2009), "Comment on "Heat transfer in vacuum packed microelectromechanical system devices" [Phys. Fluids. 20, 017103 (2008)]", *Physics of Fluids*, Vol. 21, 119101.